Diurnal, seasonal, and annual trends in atmospheric CO_2 at southwest London during 2000-2012: Wind sector analysis and comparison with Mace Head, Ireland.

*Ivan Y. Hernández-Paniagua[1], David Lowry[1], Kevin C. Clemitshaw[1], Rebecca E. Fisher[1], James L. France[1], Matthias Lanoisellé[1], Michel Ramonet[2] and Euan G. Nisbet[1]**

[1]Department of Earth Sciences, Royal Holloway, University of London, Egham, Surrey, TW20 0EX, United Kingdom, Phone +44 1784 443809. [2]Laboratoire des Sciences du Climat et de l'Environnement (LSCE/IPSL) CEA-CNRS-UVSQ, 91191 Gif-sur-Yvette, France. *Corresponding author: e.nisbet@es.rhul.ac.uk.

Abstract

In-situ measurements of atmospheric CO_2 have been made at Royal Holloway University of London (RHUL) in Egham (EGH), Surrey, UK from 2000 to 2012. The data were calibrated using NOAA calibration gases. Measured CO_2 varies on time scales that range from minutes to inter-annual and annual cycles. Seasonality and pollution episodes occur each year. Diurnal cycles vary with daylight and temperature, which influence the biological cycle of CO_2 and the degree of vertical mixing. Anthropogenic emissions of CO_2 dominate the variability during weekdays when transport cycles are greater than at weekends. Seasonal cycles are driven by temporal variations in biological activity and changes in combustion emissions. Maximum mole fractions (μmol/mol) (henceforth referred to by parts per million, ppm) occur in winter, with minima in late summer. The smallest seasonal amplitude observed, peak to trough, was 17.0 ppm CO_2 in 2003, whereas the largest amplitude observed was 27.1 ppm CO_2 in 2008.

Meteorology can strongly modify the CO_2 mole fractions at different time scales. Analysis of eight 45° wind sectors shows that the highest CO_2 mole fractions were recorded from the E and SE sectors. Lowest mole fractions were observed for air masses from the S and SW. Back-trajectory and meteorological analyses of the data confirm that the dominant sources of CO_2 are anthropogenic emissions from London and SE England. The largest annual rate of increase in the annual average of CO_2, 3.26 ppm yr^{-1} (p<0.05), was for the W sector whereas the smallest increase, 2.56 ppm yr^{-1} (p<0.05), was for the E sector. Calm winds showed an annual growth rate of 1.16 ppm yr^{-1} CO_2 (p<0.05). The EGH site shows an average growth rate of 2.5 ppm yr^{-1} CO_2 (p<0.05) over the measured period, which exceeds the observed global trend and contrasts with the decrease in CO_2 emissions reported in UK greenhouse gas inventories. This is presumably because the region has had higher growth in combustion emissions than the global average, though the low growth rate in calm

weather implies the local emissions have grown more slowly. The seasonal cycle at EGH had larger amplitudes than those recorded at the Mace Head Atmospheric Research Station (MHD) on the W coast of Ireland. Overall, the growth rate observed in annual average CO_2 at EGH was larger than that at MHD by about 0.5 ppm yr^{-1}.

Keywords

Carbon dioxide, seasonal variation, long-term trend.

1. Introduction

There are very few long-term high-quality records of urban CO_2. Time-series analyses have been used extensively to study changes in CO_2 cycles and long-term trends, but nearly all long-term records of greenhouse gases are from remote background locations in the marine boundary layer or at high altitude such as Mauna Loa or South Pole. Although several continuous records of CO_2 have been reported, only a few address the emissions of a megacity. In part this is because of the complexity of the problem: urban emissions can vary dramatically both spatially and from hour to hour.

The purpose of this report is to show that long-term observations in urban and suburban settings are indeed valuable. Well-located observation time-series in peri-urban settings can be used to provide powerful insights into urban and regional emissions, their diurnal and seasonal dynamics, and also to track the effectiveness of policy initiatives to manage CO_2 emissions. Time-series analyses of CO_2 mole fractions can provide the basis to understand fluctuations in the global carbon cycle, however very few long-term times series have been reported in heavily populated emissions 'hotspots'. Yet unless CO_2 mole fractions in populated regions are measured and understood, the efficacy of government policy initiatives cannot be independently tested and verified, nor can local and regional changes in response to emission abatement strategies and policies be tracked.

Meteorological parameters such as temperature, wind speed and direction, air mass origin and boundary layer height influence atmospheric CO_2 mole fractions. Peri-urban monitoring stations such as EGH, which is situated upwind to the prevailing wind and between a megacity and the rural environment, receive polluted urban air masses that contain high CO_2 loading, and also background air masses from less polluted sectors. The location permits study of both semi-rural and urban areas contributions to the CO_2 The direct effects of low wind speeds and a temperature inversion cap are that local emissions are dispersed slowly, remain close to the ground, and accumulate (Worthy et al., 1994). Low wind speeds are also

typically accompanied by rapidly fluctuating wind directions. Consequently, under such conditions, CO_2 data exhibit large standard deviations, as local emissions are sporadically sampled.

This study presents 13-years of continuous measurements of atmospheric CO_2 recorded at EGH from 2000 to 2012. The data set contains features of a semi-rural and an urban site, depending on air mass trajectories, which allows a complete assessment of both semi-rural and urban inputs to the CO_2 atmospheric build-up, which only very few reports have assessed. Results of the analysis and interpretation of daily and seasonal cycles, and long-term trends are compared with those observed at the MHD monitoring station. The influence on observed CO_2 annual growth rates of air mass origins at the EGH site was also evaluated.

The Egham results are set in a global context of increasing CO_2. Britain is attempting to reduce its greenhouse gas emissions. If the policy is successful, then London and SE English CO_2 mole fractions would be expected to grow more slowly than the global increase. Measurements of atmospheric CO_2 made in recent decades at monitoring stations at different latitudes, especially the key marine background observatories of the US National Oceanic and Atmospheric Administration (NOAA), have shown a dramatic and rapid rise in CO_2 levels (Thoning et al., 1989; Nakazawa et al., 1991; Dettinger et al., 1998, Haszpra et al., 2008; Zhang et al., 2013a). During the last decade, CO_2 growth has increased at a rate more than twice that of the increase observed during the 1960s (IPCC, 2013). In 2013, the global average concentration of CO_2 was 396.48 ppm (Tans et al., 2014). More specifically, the Atlantic is the source of the main prevailing wind, and thus the Egham record should be tested against the Atlantic background record, for example at Mace Head, Ireland.

2. Measurements and data

2.1 Egham site location and data

Measurements of atmospheric CO_2 were made from 2000 to 2012 at the Greenhouse Gas Laboratory of the Earth Sciences Department (GGLES) at RHUL (i.e. the EGH site). The EGH site is situated in Surrey, UK (51°25’35.99” N, 0°33’39.66” W), approximately 32 km WSW of Central London on the first significant incline (Figure 1). The EGH site is about 45 m above sea level, and 30 m above the nearby Thames Floodplain. Air is sampled from an inlet manifold located on the roof of the Earth Sciences building, approximately 15 m above ground level. The EGH site lies approximately 7 km SW of London Heathrow Airport and is ideal for local, regional, and background studies of air pollution. Windsor Great Park which is a mix of forested and agricultural land, is located around 2 km W of the site, and covers an

111 area of some 30 km^2. To the SW is a predominantly sub-urban area of clusters of housing
112 interspersed with woodland and the Surrey heathlands. The E sector is dominated by the
113 Greater London conurbation (Lowry et al., 2001).
114
115 **2.2 Sampling methodology, instrumentation and calibration**
116 CO_2 was measured continuously at the EGH site at time-intervals of 5 mins to 10 secs
117 during January 1st 2000 to December 31st 2012. Between 2000 and 2009, a LiCor 6252 non
118 dispersive infrared analyser was used to measure CO_2 (Table 1). This instrument was
119 operated in absolute mode with the reference cell filled with zero air and scrubbed with soda
120 lime to maintain 0 ppm CO_2 in the cell. Before 2007, data were logged at 5-min intervals, but
121 after 2007 data were logged at 1-minute intervals to be more consistent with European
122 stations in the GeoMon project (GeoMon, 2014). During 2009, a Picarro G1301 cavity
123 ringdown spectrometer (CRDS) was run in direct comparison with the LiCor instrument,
124 before becoming the primary instrument to measure CO_2 from 2010 to the present. Very
125 good agreement was observed between records (gradient=1.0045, intercept=-1.8678,
126 r=0.9990, p<0.001). The CRDS outputs a CO_2 measurement at approximately 10-second
127 intervals and these are 1-minute averaged. Both instruments were calibrated using NOAA
128 calibration gases.
129
130 From 2000 to 2007 two standards of 372.1 and 420.1 ppm CO_2 were analysed daily to
131 account for drift and span corrections. In 2008 the 372.1 ppm CO_2 standard was replaced by
132 a 378.9 ppm calibration gas, and in 2010 the 420.1 ppm standard replaced by a 415.4 ppm
133 calibration gas. The CRDS was calibrated during 2010 and 2011 using the replacement
134 NOAA gases. Since 2012, air standards with 380.3, 394.9 and 420.1 ppm CO_2, that were
135 prepared at MPI-Jena and calibrated against NOAA standards as part of the IMECC project
136 (IMECC, 2014), have been analysed weekly.
137
138 Wind direction, wind speed and temperature were recorded from 2000 to 2006 using a MJP
139 Geopacks PC weather station, which was replaced in 2007 by a Geopacks WS-200 MK-III
140 weather station.
141
142 **2.3 Mace Head Research Station and data**
143 The Mace Head station (53°20' N, 9°54' W) samples Atlantic background air. MHD is
144 situated on the Atlantic Ocean coastline of Ireland to monitor CO_2 mole fractions and
145 quantify European and trans-Atlantic sources and sinks of CO_2 (Bousquet et al., 1996;
146 Derwent et al., 2002; Messager et al., 2008). It receives clean maritime air masses from
147 across the Atlantic Ocean, and under anti-cyclonic conditions, air masses from the UK and

continental Europe (Derwent et al., 2002). The MHD CO_2 data set is maintained by the Climate and Environment Sciences Laboratory (LSCE), which belongs to the Institut Pierre Simon Laplace, and was obtained from the web site of the World Data Centre for Greenhouse Gases of the World Meteorological Organisation (http://ds.data.jma.go.jp/gmd/wdcgg). The data set spans continuous, hourly, measurements of CO_2 from January 1992 to December 2011.

2.4 Meteorology at the EGH site

The climate at EGH is mild and maritime, with widely varying wind directions. SW winds are most common as depressions track across the UK, but E winds are frequent in anti-cyclonic conditions. NE winds occur regularly in winter and summer. Relatively clean air arrives at the sampling site from the SW and SSW. In background conditions, air pollutant mole fractions are close to those recorded for contemporaneous Atlantic background air measured at MHD, Ireland (Lowry et al., 1998). By contrast, E air trajectories pass over the whole London urban area (8.17 million people; ONS, 2011) before arrival at the site.

During slow-moving anti-cyclonic air conditions in winter and early spring, the initial relatively clean air is augmented by emissions from the London basin. Such widespread conditions may persist for several days or more, with primary air pollutants accumulating as the blanketing temperature inversion rises and falls (Lowry et al., 1998: LAQN, 2014), and thus CO_2 data recorded at EGH may be regarded as a broad proxy for air quality in the London area. Trajectories for SW air streams typically approach above the English Channel and descend over 80-100 km of rural and sub-urban areas before reaching EGH. Air masses from the NE often pass over the North Sea from Arctic regions, then over 80-100 km of rural East Anglia before reaching NW London and on to EGH (Lowry et al., 2001).

Figure 2 shows the frequency of counts of measured wind direction occurrence by season during 2000-2012. Overall, the predominant wind direction at the study site was SW, occurring 21% of the time. Calm conditions (half hour averages) of wind speeds less than 0.1 m s^{-1} occurred 17.7% of the time. Significant seasonal variations in frequency were observed for NE winds between winter and summer. Interestingly, the fewest calm winds occurred in winter (11.5%, 7,783 events), while the most were observed in autumn (23.1%, 16,256 events).

2.5 Definition of wind sectors and seasons

To enable wind-sector analyses, the data set was divided into 8 wind sectors of 45° starting from 0° ± 22.5°. To avoid data duplicity, the lower bound of each sector was established by

adding 0.5°. To carry out seasonal analyses, 4 seasons were defined according to temperature records in the northern hemisphere: winter (December to February), spring (March to May), summer (June to August) and autumn (September to November).

2.6 Data quality and capture rate

Although occasional instrument breakdowns caused data gaps, the data capture varied between 89-99% of maximum possible yearly measurements. The total percentage coverage is shown in Figure 3. A data capture threshold of 75% was used to consider data valid (Zellweger et al., 2009). 30-min averages were used to calculate daily averages. Monthly averages were calculated from daily averages whereas yearly averages were calculated from monthly averages. Wind speed data coverage was from 67-99%, wind direction from 76-99% and temperature from 91-99% (Figure 3).

2.7 Data analyses

The dataset was analysed extensively with the *openair* package (Carslaw et al., 2012) for R software (R Core Team, 2013). Long-term trends were computed with the MAKESENS 1.0 macro, which performs two types of statistical analysis. Firstly, the presence of a monotonic increasing or decreasing trend was tested with the non-parametric Mann-Kendall test. Secondly, slopes of linear trends were calculated with the non-parametric Sen's method. MAKESENS used the normal approximation test for n = 13 at EGH to test the presence of a statistically significant trend using the Z value. A positive Z value indicates an increasing trend, with a negative value indicative of a decreasing trend. To test for monotonic trends, a two-tailed test at a level of significance *of* α was used. H_0 was rejected if the absolute value of Z was greater than $Z_{1-\alpha/2}$ obtained from standard normal cumulative distribution tables. MAKESENS tests significance levels of α of 0.001, 0.01, 0.05 and 0.1 (ie p values of 99.9, 99, 95 and 90%, repectively) (Salmi et al., 2002).

Sen's method was used where the trend is assumed to be linear and can be represented by a slope and a constant Q and B, respectively. To calculate Q, first the slopes of all data values were calculated in pairs. For n values x_j in the time series, $N = n(n-1)2$ slope estimates were obtained Q_i. The Sen's estimator of slope is the median of these N values of Q_i. Then, the N values of Q_i were ranked from the smallest to the largest. A $100(1-\alpha)\%$ two-sided confidence interval about the slope estimate was obtained by the non-parametric technique based on the normal distribution. MAKESENS computes the confidence interval at two different confidence levels; $\alpha = 0.01$ and $\alpha = 0.05$, resulting in two different confidence intervals. To obtain an estimate of B, the n values of differences $x_i - Qt_i$ were calculated. The median of these values gives an estimate of B (Salmi et al., 2002).

The Seasonal-Trend Decomposition technique (STL) was used to decompose the time-series into trend, seasonal and residual components (Cleveland et al., 1990). STL consists of two recursive procedures: an inner loop nested inside and outer loop. In each of the passes through the inner loop, the seasonal and trend components are updated once; each complete run of the inner loop consists of $n_{(i)}$ such passes. Each pass of the outer loop consists of the inner loop followed by a computation of the robustness weights; these weights are used in the next run of the inner loop to reduce the influence of transient, aberrant behaviour on the trend and seasonal components. An initial pass of the outer loop is carried out with all robustness weights equal to 1, and then $n_{(0)}$ passes of the outer loop are carried out. SPSS 19.0 for Windows was used to perform statistical analyses.

3. Results and discussion

3.1 CO_2 Continuous measurements from 2000 to 2012 at EGH

Seasonal cycles, winter pollution episodes and an increasing trend were observed in the data set. The seasonal cycle shows the largest CO_2 mixing ratios in winter and the lowest in late summer (Figure 4a). This cycle arises from a combination of CO_2 uptake by photosynthesis (Nakazawa et al., 1991; Dettinger et al., 1998), which is enhanced during the summer when the lowest CO_2 mole fractions were recorded, and increased emissions from fossil fuel burning for heating during winter. Winter pollution episodes can be caused by strong surface radiation inversion trapping local emissions, the breakdown of this inversion with subsequent transport of CO_2 from aloft to the surface, and long-range transport of CO_2 from continental Europe to EGH. The increasing overall trend is in accordance with that observed worldwide; the increment in the CO_2 atmospheric levels is mainly due to the combustion of fossil fuels (Ramonet et al., 2010; Tans et al., 2014).

Daily averages of CO_2 calculated from 30-minute averages are plotted in Figure 4b. A high proportion of daily values were close to background mole fractions (data not shown) due to the high prevalence of westerly winds. Interestingly, although their maximum mole fraction increased, the frequency and amplitude of spikes (defined as $>3\sigma$) decreased during the period studied, which may be due to the introduction of more efficient vehicle engines spurred by an increase in fossil fuel costs.

3.2 Daily profiles and weekly cycles

Hourly averages were calculated from the 30 min averages. Diurnal variations were calculated using normalised daily cycles derived from average diurnal cycles by subtracting or adding daily averages in order to remove the impacts of long-term trends (Zhang et al.,

2013b). Diurnal variations split by seasons are plotted in Figure 5. The largest daily amplitude value (AV_d) of 26.3 ppm CO_2 occurs in summer with a peak at 05:00 GMT and trough at 14:00 GMT; the smallest AV_d of 10.2 ppm CO_2 is in winter with a peak at 09:00 GMT and a trough at 14:00 GMT. The larger AV_d in summer is due to an enhanced biological (photosynthesis-respiration) system with more abundant vegetation in the 'green belt' around EGH. By contrast, in winter, the predominance of deciduous trees and slower growth of vegetation produces the smallest diurnal AV_ds. The morning peak of CO_2 on top of the daily cycle, particularly in winter, highlights the role of the planetary boundary layer height driving the CO_2 mole fractions.

At EGH, an average AV_d of 17.0 ppm CO_2 was calculated for the 13-year averaged daily cycle. A similar winter AV_d of 7 ppm CO_2 was recorded at the rural site of Hegyhátsál, Hungary. However at EGH, the summer AV_d of 26 ppm CO_2 is half of 52 ppm CO_2 calculated in summer by Haszpra et al. (2008), which highlights differences in the biological system in the continental interior and the maritime-moderated climate of EGH. At an urban location in Basel, Switzerland, the summer AV of 61 ppm CO_2 reported by Vogt et al. (2006) is much higher than that at EGH. The Basel station is greatly affected by traffic load and wind speed conditions leading to a higher variability than at EGH, but has also a greater annual temperature variation to exacerbate the biological system.

The normalised daily cycle shows the largest CO_2 mole fractions at EGH before sunrise (Figure 5), the earliest being at 05:00 GMT in summer and the latest at 09:00 GMT in winter. The peaks in the CO_2 cycle appear before the biological system becomes a net CO_2 sink and are enhanced by shallow night-time boundary layers (Haszpra et al., 2008; Larson and Volkmer, 2008). Also, vegetation respiration contributes to atmospheric CO_2 as maximum biological activity occurs before sunrise, hence the peak in the CO_2 cycle follows the timing of sunrise during the year. Boundary layer break up, vertical mixing after sunrise and the onset of net biological CO_2 uptake enhance the AVs and leading to cycle minima at EGH at 14:00 GMT due to the biological system. This is observed clearly in summer when the vegetation uptake reaches its maximum activity (Haszpra et al., 2008).

3.3 Seasonal cycles from filtered data (STL)

CO_2 molar fractions respond to changes in temperature, vegetation extent, combustion emissions and meteorology. Seasonal cycles were obtained by filtering the data set with STL at EGH (Figure 6a). The shape of the cycles is similar each year, with winter maxima and summer minima. Maxima, are observed in January in 2000 and 2001, in December from 2002 to 2009, and in November from 2010 to 2012. By contrast, apart from 2003 (June) and

2006 (July), minima are consistently seen in August. Shoulders in the cycles are observed in February due to the prevalence of higher W wind speeds than in January and March. The advection of background westerly air masses generates convective conditions that disperse local emissions, and dilute the CO_2 accumulated by mixing it with clean air.

The average seasonal amplitude value (AV_s) was calculated using STL for the 13-year record as 21.7 ± 3.4 (1σ) ppm CO_2. The lowest AV_s was 17.0 ppm in 2003 with the largest of 27.1 ppm in 2008. Despite annual variability in the AV_s, a statistically significant (*p=0.005*) annual growth rate of 0.64 ppm CO_2 yr^{-1} in AV_s was obtained (Figure 6b). This increasing and variable trend in AV_s observed agrees with several previous studies (Cleveland et al., 1983; Thoning et al., 1989; Dettinger et al., 1998), although at EGH the larger growth rate in AV_s observed is strongly influenced by inter-annual variability. This growth rate may be a result of increased photosynthetic activity (perhaps in part in response to increasing atmospheric CO_2 mole fractions), increases in fossil fuel combustion and to a lesser extent to changes in ocean and land temperatures (Cleveland et al., 1983; Dettinger et al., 1998; Barichivich et al., 2012; 2013).

The onset of the growing season in the northern hemisphere, and thus CO_2 uptake are strongly coupled with temperature (Haszpra et al., 2010; Barichivich et al., 2012; 2013). Monthly de-trended averages of CO_2 and temperature were obtained from the dataset using the STL filtering technique (Figure 6). Results show a strong anti-phase relationship of the seasonal cycles of CO_2 and temperature with linear regression analysis confirming a negative correlation with an r value of 0.90 and significance of *p<0.001* for 156 monthly averages. Temperature increases also modify the CO_2 AV_s by increasing respiration rates, enhancing CO_2 release, and prolonging the growing season and thereby increasing CO_2 uptake from the atmosphere (Piao et al., 2008). A linear relationship was observed between minimum CO_2 mole fractions and maximum temperatures in summer (r=0.71, p<0.01), but was not observed for CO_2 maximum mole fractions and temperature minimum values in winter (r=0.06, p>0.05), which highlights the dominant role of the planetary boundary layer height and its evolution during the year on the CO_2 mole fractions recorded (PORG, 1997).

3.4 Secular trend and residuals (STL)

Figure 7 shows the CO_2 secular trend and residuals recorded at EGH during 2000-2012. The smoothed line of the secular trend was computed by filtering the data set with the STL technique (Cleveland et al., 1990). Residuals represent irregular variations beyond the seasonal cycles and secular trend. The smoothed curve shows persistent increases in the CO_2 mole fractions with declines in 2004 and 2008. The declines at EGH both coincide with

observations from monitoring stations across the globe (Tans et al., 2014), and are explained by two factors: 1) a global increase in temperatures during 2003 and 2004, which may have led to increased uptake by vegetation, and; 2) during 2008-2009, the global economic crisis and high oil prices caused a 50% reduction in the annual increase in global emissions of CO_2. That is in good agreement with data from the UK GGI (2014) that reports a decline in CO_2 emissions from the business, residential and industrial processes sectors during 2008-2009.

3.5 Growth rate estimated by wind sector at Egham

CO_2 annual growth rates were calculated by wind sector. The data set was split into 8 wind sectors and Sen's estimate (Salmi et al., 2002) was applied to calculate the growth rate per sector. The growth rates obtained are listed in Table 2 and range from 2.56 ppm CO_2 yr^{-1} (E) to 3.26 ppm CO_2 yr^{-1} (W), with a significance of $p<0.01$ obtained for all wind sectors. The largest growth rate in the W sector may be due to new combustion sources in that sector. The calm sector shows an annual growth rate of 1.16 ppm CO_2 yr^{-1}, which can in part be attributed to the decreasing trend in CO_2 emissions reported for the region close to the EGH measurements site in the UK NAEY inventory (NAEI, 2013A study of methane at the EGH site (Lowry et al., 2001), suggested that the local source footprint was maximum 3-4 km from site. Since this study there have been significant decreases in CH_4 and CO_2 due to closure of a local landfill site. From recording CO_2 at least 10 ppm higher than the classified wind sectors, the calm sector now has annual averaged CO_2 close to those for the Eastern quadrant.

3.6 Mace Head comparison

Figure 8 compares unfiltered monthly averages of CO_2, calculated from daily averages, at EGH and MHD for 2000-2011. The relatively high EGH results are due to local emissions and air masses from Greater London, whereas the MHD observations show mostly background Atlantic Ocean levels. Differences in monthly averages between the two sites ranged from 0.2 to 36.1 ppm CO_2. The smallest differences are always observed in late spring and early summer, which coincides with the onset of the growing season at EGH when vegetation becomes a net sink for CO_2 (Haszpra et al., 2008, Barichivich et al., 2013). By contrast, the biggest differences are always found in winter, when the largest monthly CO_2 mole fractions are observed at EGH due to the combination of increased combustion sources and presumably soil respiration, and frequency of anti-cyclonic weather conditions (Worthy et al., 1994).

Normalised weekly cycles were calculated using hourly averages relative to the weekly mean. Figure 9 shows the normalised weekly cycles at EGH and MHD with larger amplitudes (peak-to-trough) seen at EGH. Daily amplitudes range from 15.2 to 19.3 ppm CO_2 at EGH and from 2.0 to 2.3 ppm CO_2 at MHD. Significant variability at EGH was observed at EGH between weekdays and weekends (2.3 ppm CO_2 on average larger in weekends) with lower minimum mole fractions on weekends but was not observed at MHD. It is clear that during weekdays CO_2 emissions in the sub-urban area are greater than at weekends. The process of respiration/uptake by vegetation does not change during the week in the normalised cycles; the higher mole fractions are thought to be caused by combustion gases emitted (e.g. heating) near to EGH, in Greater London and on the very busy motorways and main road network (Kotthaus et al., 2012). As with the daily cycle, the day of week peaks coincide with sunrise (between 04:00 and 08:00 GMT depending on the season) with the trough in early afternoon (14:00 GMT).

By contrast, the daily cycle at MHD does not show significant changes between different days of the week. The small variations observed in clean sector data at MHD indicate that the site is not influenced by major CO_2 sources or sinks and the CO_2 cycle from local vegetation is clean sector data dampened by the reduced development of inversion conditions at this coastal site (Dettinger et al., 1998; Derwent et al., 2002; Haszpra et al., 2010). Variations in seasonal cycles of CO_2 have been reported for sites with local vegetation and combustion sources, whereas more remote locations normally show more harmonic cycles (Nakazawa et al., 1991; Dettinger et al., 1998).

3.7 Seasonal cycles comparison

Seasonal cycles for CO_2 at MHD were computed from monthly averages using the STL technique (Cleveland et al., 1990), and are shown in Figure 10a. The annual cycles remained almost constant with much less variability than at EGH. An anomaly or small trough at the maximum of the cycle occurred each February in 2000 to 2004, and are attributed to dilution by air masses with relatively high wind speeds. CO_2 AV_s range from 12.9 to 14.6 ppm CO_2 (Figure 10b). There is no trend in the CO_2 AV_s during 2000-2011 at MHD whereas at EGH a linear increasing of 0.64 ppm CO_2 yr^{-1} (p<0.05) was found. This increase is related to new local CO_2 combustion sources, which increase CO_2 in winter, and enhanced uptake of CO_2 by vegetation during summer.

3.8 CO_2 long-term trends at EGH and MHD from 2000 to 2011

Annual CO_2 averages at EGH and MHD were calculated from monthly averages and are plotted in Figure 11a. Overall, a total increment of 28.1 ppm CO_2 is observed at EGH for

2000-2011, with an increment of 22.4 ppm is observed at MHD. Annual variability is evident: at EGH annual changes in annual averages (ΔCO_2) range from -0.6 (2006-2007) to 7.8 ppm (2001-2002), whereas at MHD ΔCO_2 ranges from 1.0 (2007-2008) to 3.1 ppm (2000-2001). Interestingly, the largest ΔCO_2 at EGH and MHD coincide (in 2000 to 2001), but the smallest ΔCO_2 at MHD does not coincide with that at EGH.

The Mann-Kendall test and Sen's estimate (Salmi et al., 2002) were used to calculate trends in annual averages at EGH and MHD, as shown in Figure 11a. Statistically significant (p<0.01) average growth rates of 2.5 and 1.9 ppm yr^{-1} were calculated at EGH and MHD, respectively. Annual residuals, defined as the difference of annual averages minus the Sen's estimates, ranged from -2.9 ppm CO_2 (2000) to 3.1 ppm CO_2 (2007) at EGH, and from -1.0 ppm CO_2 (2000) to 0.7 ppm CO_2 (2002) at MHD. The largest residuals observed at EGH and MHD are 3.1 ppm CO_2 in 2007 and 0.7 ppm CO_2in 2002, respectively, whereas the lowest residuals at EGH of -2.9 ppm CO_2 and at MHD of -1.0 ppm CO_2 coincided in 2000.

The increasing trends in CO_2 annual averages observed at EGH and MHD agree well with those at other monitoring stations, and confirm the rate of increasing CO_2 mole fractions around the globe (Haszpra et al., 2008; Ramonet et al., 2010; Barichivich et al., 2013; Zhang et al., 2013a; Tans et al., 2014).

3.9 Comparison with the UK National Emissions Inventory (UK NAEI)

The UK NAEI reports that during 2000-2012, CO_2 emissions decreased by ca.14.2% (NAEI, 2014). By contrast, the EGH data show that during the period 2000-2012, atmospheric CO_2 increased by 8.4%. For comparison, during the slightly shorter 2000-2011 period, CO_2 at Mace Head rose by 6%, which agrees with upward trends recorded at several locations in Europe during 2000-2005 (Ramonet et al., 2010). All other factors being equal, this would imply that in the London region, CO_2 emissions have risen in excess of the increase in the regions contributing to the Atlantic background values (i.e. global but particularly USA). Interestingly, airborne CO_2 measurements in the Greater London Area suggest that the UK NAEI underestimates CO_2 emissions by a factor of 2.3 (O'Shea et al., 2014), whereas annual estimates of net exchange of CO_2 above Central London agree with the UK NAEI estimates (Helfter et al., 2011).

Ramonet et al. (2010) attribute the observed upward trends in CO_2 to two possible causes: boundary layers becoming more shallow, and regional changes in CO_2 emissions within 500 km of the measurement locations, which account for 32% and 27%, respectively, of the

trends. By contrast, Aulagnier et al. (2009) suggest a combination of the more shallow boundary layers and changes in wind speed. However, it is clear that further measurements of CO_2 and other tracers for anthropogenic emissions such as $^{13}CO_2$, $^{14}CO_2$ and CO, wind speed and direction, and boundary layer height are required to verify the origins of the trends observed. A limiting factor is the uncertainty of 2% in the regional emissions of CO_2 that may obscure other processes (NAEI, 2014).

4. Conclusions

Continuous high-precision and high-frequency CO_2 data recorded at EGH and MHD monitoring stations were used to estimate CO_2 growth rates from 2000 to 2012, and from 2000 to 2011, respectively. CO_2 mole fractions varied on time scales ranging from minutes to inter-annual and annual cycles. The greatest mole fractions were recorded for winds from the E and SE sectors, representing CO_2 transported from anthropogenic sources in the London region and continental Europe. The lowest mole fractions were observed for the S and SW sectors, where air travels from the Atlantic Ocean over a maximum of 100-150 km of semi-rural England.

The diurnal cycle of CO_2 varies with patterns of atmospheric transport and heating, and biologically with length of daylight. Weekly cycles are strongly influenced by anthropogenic emissions during weekdays when fossil fuel burning and combustion processes are higher than at weekends. Seasonal cycles are driven by temporal variations in human behaviour, atmospheric transport and in photosynthesis. Annual cycles at EGH and MHD exhibit maxima and minima in winter and late summer, respectively. The smallest seasonal amplitude of CO_2 observed at EGH was 17.0 ppm CO_2 in 2003, with the largest of 27.1 ppm CO_2 in 2008. This underlies an increasing trend in seasonal amplitudes observed at other northern hemisphere locations.

An annual averaged growth rate of 2.45 ppm CO_2 yr^{-1} (p<0.05) was calculated for EGH during 2000-2012 compared with 1.9 ppm CO_2 yr^{-1} (p<0.05) for MHD between 2000 and 2011. The larger growth rate observed at EGH was due to local and regional increases in CO_2 emissions from fossil fuel combustion that are not recorded in the MHD data set. The CO_2 increasing trend observed is opposite to the decreasing trend in CO_2 emissions reported in the UK NAEI, however the uncertainty in CO_2 emissions estimations still remains at a few per cent. More continuous long-term measurements of CO_2, particularly in regions of high emissions, are required to better understand the growth rate. This work demonstrates the usefulness of long-term CO_2 monitoring close to major emissions 'hot-spots' in order to measure emissions in highly populated areas, and to test the validity of 'bottom-up' inventory

assessment. The measurement and analysis reported here permit wholly independent testing and verification of the UK national inventory data for emissions.

5. Acknowledgements

Grant-aided support to I.Y. Hernandez-Paniagua from the Mexican National Council of Science and Technology (CONACYT, scholarship number 215094) and Public Education Ministry (SEP) is gratefully acknowledged. The CO_2 measurement record at Egham has been sustained since 1996 by D. Lowry, supported by N.D. Rata, C. W. Holmes, P. O'Brien, S. Sriskantharajah, R.E. Fisher, J.L. France, and M. Lanoisellé, in a group led by E.G. Nisbet. Support for the CO_2 measurements has been from Royal Holloway, and also in part from the European Commission's IMECC (2007-10) and GEOMON (2007-11) projects.

References

Aulagnier, C., Rayner, P., Ciais, P., Vautard, R., Rivier, L., Ramonet, M. (2010). Is the recent build-up of atmospheric CO_2 over Europe reproduced by models. Part 2: An overview with the atmospheric mesoscale transport model CHIMERE. *Tellus, Series B: Chemical and Physical Meteorology,* 62(1), 14-25.

Barichivich, J., Briffa, K.R., Osborn, T.J., Melvin, T.M., Caesar, J. (2012). Thermal growing season and timing of biospheric carbon uptake across the northern hemisphere. *Global Biogeochemical Cycles,* 26(4), GB4015.

Barichivich, J., Briffa, K.R., Myneni, R.B., Osborn, T.J., Melvin, T.M., Ciais, P., Piao, S., Tucker, C. (2013). Large-scale variations in the vegetation growing season and annual cycle of atmospheric CO_2 at high northern latitudes from 1950 to 2011. *Global Change Biology,* 19(10), 3167-3183.

Bousquet, P., Gaudry, A., Ciais, P., Kazan, V., Monfray, P., Simmonds, P., Jennings, S., O'Connor, T. (1996). Atmospheric CO_2 concentration variations recorded at Mace Head, Ireland, from 1992 to 1994. *Physics and Chemistry of the Earth*, 21(5-6), 477-481.

Carslaw, D.C., Ropkins, K. (2012). openair - An R package for air quality data analysis. *Environmental Modelling and Software*, 27-28, 52-61.

Cleveland, W.S., Freeny, A.E., Graedel, T.E. (1983). The seasonal component of atmospheric CO_2: Information from new approaches to the decomposition of seasonal time series (Mauna Loa, Hawaii, South Pole). *Journal of Geophysical Research,* 88(C15), 10934-10946.

513 Cleveland, R.B., Cleveland, W.S., McRae, J., Terpenning, I. (1990). STL: a seasonal-trend
514 decomposition procedure based on Loess. *Journal of Official Statistics*, 6(1), 3-33.

515 Derwent, R.G., Ryall, D.B., Manning, A., Simmonds, P.G., O'Doherty, S., Biraud, S. (2002).
516 Continuous observations of carbon dioxide at Mace Head, Ireland from 1995 to 1999 and its
517 net European ecosystem exchange. *Atmospheric Environment*, 36(17), 2799-2807.

518 Dettinger, M.D., Ghil, M. (1998). Seasonal and interannual variations of atmospheric CO_2
519 and climate. *Tellus, Series B: Chemical and Physical Meteorology*, 50(1), 1-24.

520 Global Earth Observation and Monitoring of the Atmosphere (GeoMon). Available at:
521 http://www.geomon.eu/index.php/en/. Last access: 12-May-2014.

522 Haszpra, L., Barcza, Z., Hidy, D., Szilagyi, I., Dlugokencky, E., Tans, R. (2008). Trends and
523 temporal variations of major greenhouse gases at a rural site in Central Europe.
524 *Atmospheric Environment*, 42(38), 8707-8716.

525 Haszpra, L., Barcza, Z. (2010). Climate variability as reflected in a regional atmospheric CO_2
526 record. *Tellus, Series B: Chemical and Physical Meteorology*, 62(5), 417-426.

527 Helfter, C., Famulari, D., Phillips, G.J., Barlow, J.F., Wood, C.R., Grimmond, C.S.B.,
528 Nemitz, E. (2011). Controls of carbon dioxide concentrations and fluxes above central
529 london. *Atmospheric Chemistry and Physics,* 11(5), 1913-1928.

530 Infrastructure for Measurements of the European Carbon Cycle (IMECC). Available at
531 http://imecc.ipsl.jussieu.fr/. Last access: 12-May-2014.

532 IPCC, 2013: *Climate Change 2013: The Physical Science Basis. Contribution of Working*
533 *Group I to the Fifth Assessment Report of the Intergovernmental Panel on Climate Change*
534 [Stocker, T.F., D. Qin, G.-K. Plattner, M. Tignor, S.K. Allen, J. Boschung, A. Nauels, Y. Xia, V.
535 Bex and P.M. Midgley (eds.)]. Cambridge University Press, Cambridge, United Kingdom and
536 New York, NY, USA, 1535 pp.

537 Kotthaus, S., Grimmond, C.S.B. (2012). Identification of micro-scale anthropogenic CO_2,
538 heat and moisture sources - processing eddy covariance fluxes for a dense urban
539 environment. *Atmospheric Environment,* 57, 301-316.

540 Larson, V.E., Volkmer, H. (2008). An idealized model of the one-dimensional carbon dioxide
541 rectifier effect. *Tellus, Series B,* 60(4), 525-536.

542 London Air Quality Network (LAQN). (2014). Environmental Research Group, King's College
543 London. *Accessed on 20 August 2014. http://www.londonair.org.uk/LondonAir/Default.aspx.*

Lowry, D., O'Brien, P., Nisbet, E.G., Rata, N.D. (1998). $\delta^{13}C$ of atmospheric methane: An integrated technique for constraining emission sources in urban and background air, in *Isotope Techniques in the Study of Environmental Change*. Proceedings of IAEA Symposium, Vienna, April 1997, 57-67.

Lowry, D., Holmes, C.W., Rata, N.D., O'Brien, P., Nisbet, E.G. (2001). London methane emissions: Use of diurnal changes in concentration and delta C-13 to identify urban sources and verify inventories. *Journal of Geophysical Research*. 106, D7, 7427-7448.

Messager, C., Schmidt, M., Ramonet, M., Bousquet, P., Simmonds, P., Manning, A. Ciais, P. (2008). Ten years of CO_2, CH_4, CO and N_2O fluxes over Western Europe inferred from atmospheric measurements at Mace Head, Ireland. *Atmospheric Chemistry and Physics Discussions*, 8(1), 1191-1237. Check

Nakazawa, T., Aoki, S., Murayama, S., Fukabori, M., Yamanouchi, T., Murayama, H., Shiobara, M., Hashida, S., Kawaguchi, S., Tanaka, M. (1991). The concentration of atmospheric carbon dioxide at the Japanese Antarctic Station, Syowa. *Tellus, Series B*, 43B(2), 126-135.

NAEI (2014). The National Atmospheric Emissions Inventory. Available at http://naei.defra.gov.uk/data/. Last access: 25 May 2014.

O'Shea, S.J., Allen, G., Fleming, Z.L., Bauguitte, S.J.-B., Percival, C.J., Gallagher, M.W., Lee, J., Helfter, C., Nemitz, E. (2014). Area fluxes of carbon dioxide, methane, and carbon monoxide derived from airborne measurements around Greater London: A case study during summer 2012. *Journal of Geophysical Research D: Atmospheres,* 119(8), 4940-4952.

Office for National Statistics (ONS). 2011 Census: Key Statistics for England and Wales. Available at: http://www.ons.gov.uk/ons/rel/census/2011-census/key-statistics-for-local-authorities-in-england-and-wales/stb-2011-census-key-statistics-for-england-and-wales.html. Last access: 12-May-2014.

Piao, S., Ciais, P., Friedlingstein, P., Peylin, P., Reichstein, M., Luyssaert S., Margolis, H., Fang, J., Barr, A., Chen, A., Grelle, A., Hollinger, D.Y., Laurila, T., Lindroth, A., Richardson, A.D., Vesala, T. (2008). Net carbon dioxide losses of northern ecosystems in response to autumn warming. *Nature,* 451(7174), 49-52.

PORG, 1997. Ozone in the United Kingdom. Fourth Report of the UK Photochemical Oxidants Review Group, Department of the Environment, Transport and the Regions, London. Published by Institute of Terrestrial Ecology, Bush Estate, Penicuik, Midlothian, EH26 0QB, UK. ISBN: 0-870393-30-9.

R Core Team (2013). R: A Language and Environment for Statistical Computing. ISBN 3-900051-07-0. R Foundation for Statistical Computing. Vienna, Austria.

Ramonet, M., Ciais, P., Aalto, T., Aulagnier, C., Chevallier, F., Cipriano, D., Necki, J.N. (2010). A recent build-up of atmospheric CO_2 over Europe. Part 1: Observed signals and possible explanations. *Tellus, Series B: Chemical and Physical Meteorology,* 62(1), 1-13.

Salmi, T., Määttä, A., Anttila, P., Ruoho-Airola, T., Amnell, T. (2002). Detecting trends of annual values of atmospheric pollutants by the Mann-Kendall test and Sen's slope estimates – the Excel template application MAKESENS. *Publications on Air Quality Report code FMI-AQ-31*, (31), 1-35. Helsinki, Finland.

Tans, P., Keeling, R. (2014). NOAA/ESRL (www.esrl.noaa.gov/gmd/ccgg/trends/) and Scripps Institution of Oceanography (scrippsco2.ucsd.edu/). Last access: 12-May-2014.

Thoning, K.W., Tans, P.P. (1989). Atmospheric carbon dioxide at Mauna Loa Observatory 2. Analysis of the NOAA GMCC data, 1974-1985. *Journal of Geophysical Research*, 94(D6), 8549-8565.

UK Greenhouse Gas Inventory (UK GGI), 1990 to 2012. (2014). Annual Report for Submission under the Framework Convention on Climate Change. *Accessed on 20 August 2014. Available at https://www.gov.uk/government/publications/uk-greenhouse-gas-inventory*.

Vogt, R., Christen, A., Rotach, M.W., Roth, M., Satyanarayana, A.N.V. (2006). Temporal dynamics of CO_2 fluxes and profiles over a central European city. *Theoretical and Applied Climatology,* 84(1-3), 117-126.

Worthy, D.E.J., Trivett, N.B.A., Hopper, J.F., Bottenheim, J.W., Levin, I. (1994). Analysis of long-range transport events at Alert, Northwest Territories, during the Polar Sunrise Experiment. *Journal of Geophysical Research,* 99(D12), 25,329-25,344.

Zhang, F., Zhou, L.X. (2013a). Implications for CO_2 emissions and sinks changes in western China during 1995-2008 from atmospheric CO_2 at Waliguan. *Tellus, Series B: Chemical and Physical Meteorology,* 65(1), DOI: 10.3402/tellusb.v65i0.19576.

Zhang, F., Zhou, L., Conway, T. J., Tans, P. P., Wang, Y. (2013b). Short-term variations of atmospheric CO_2 and dominant causes in summer and winter: Analysis of 14-year continuous observational data at Waliguan, China. *Atmospheric Environment,* 77, 140-148.

Zellweger, C., Hüglin, C., Klausen, J., Steinbacher, M., Vollmer, M., Buchmann, B. (2009). Inter-comparison of four different carbon monoxide measurement techniques and evaluation

609 of the long-term carbon monoxide time series of Jungfraujoch. *Atmospheric Chemistry and*
610 *Physics,* 9(11), 3491-3503.

611

612 Table 1. Instrumentation, precision, frequency and periods used to measure CO_2 at the
613 Egham site during 2000 to 2012.

Period	Instrument	Precision	Measurement frequency
1999-2009	Licor 6252 (Non-dispersive IR)	± 0.1 ppm	1999-2006 (every 5 min) 2007-2009 (every 1 min)
2010-2012	Picarro G1301 (Cavity Ring Down Spectroscopy)	± 0.05 ppm	2010-2012 (every 10 sec)

614

615 Table 2. Averaged CO_2 growth rates for 2000-12 calculated by wind sector at the EGH site.

Sector	N	NE	E	SE	S	SW	W	NW	Calm
CO_2 growth rate (ppm yr^{-1})	3.20*	2.78*	2.56*	2.85*	2.78*	2.92*	3.26*	2.71*	1.16**

616 **Level of significance α = 0.0001*
617 ***Level of significance α = 0.1*
618

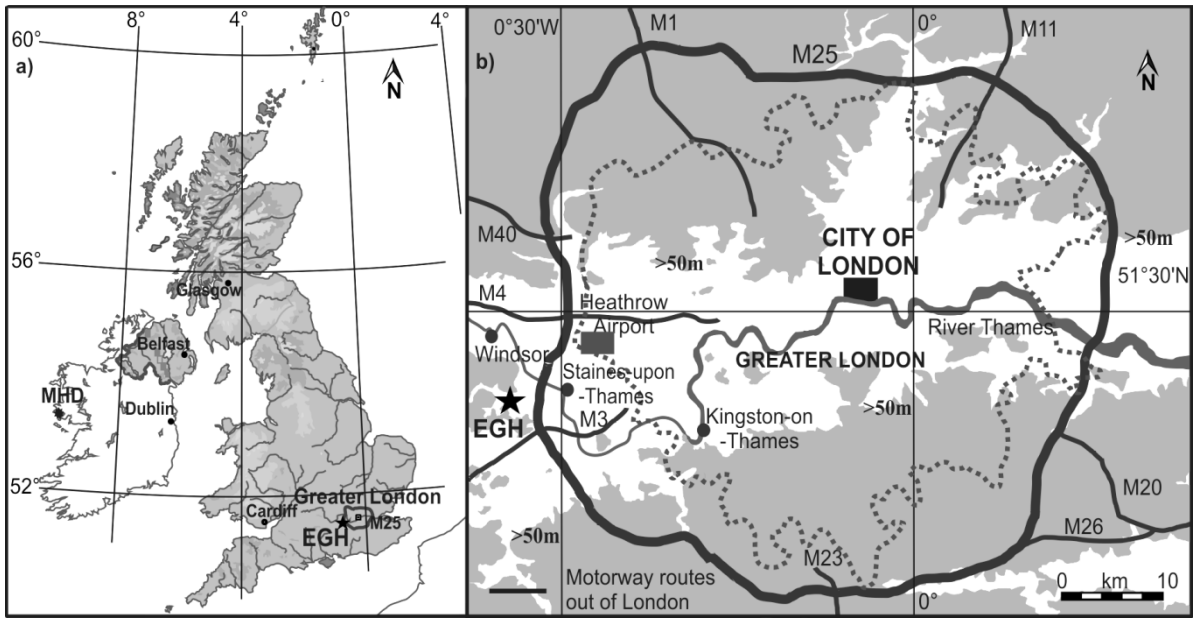

619

620 Figure 1a). The EGH site, M25 motorway and greater London area in the national context.
621 b). EGH site at RHUL in relation to central London and the Greater London motorway
622 network.
623

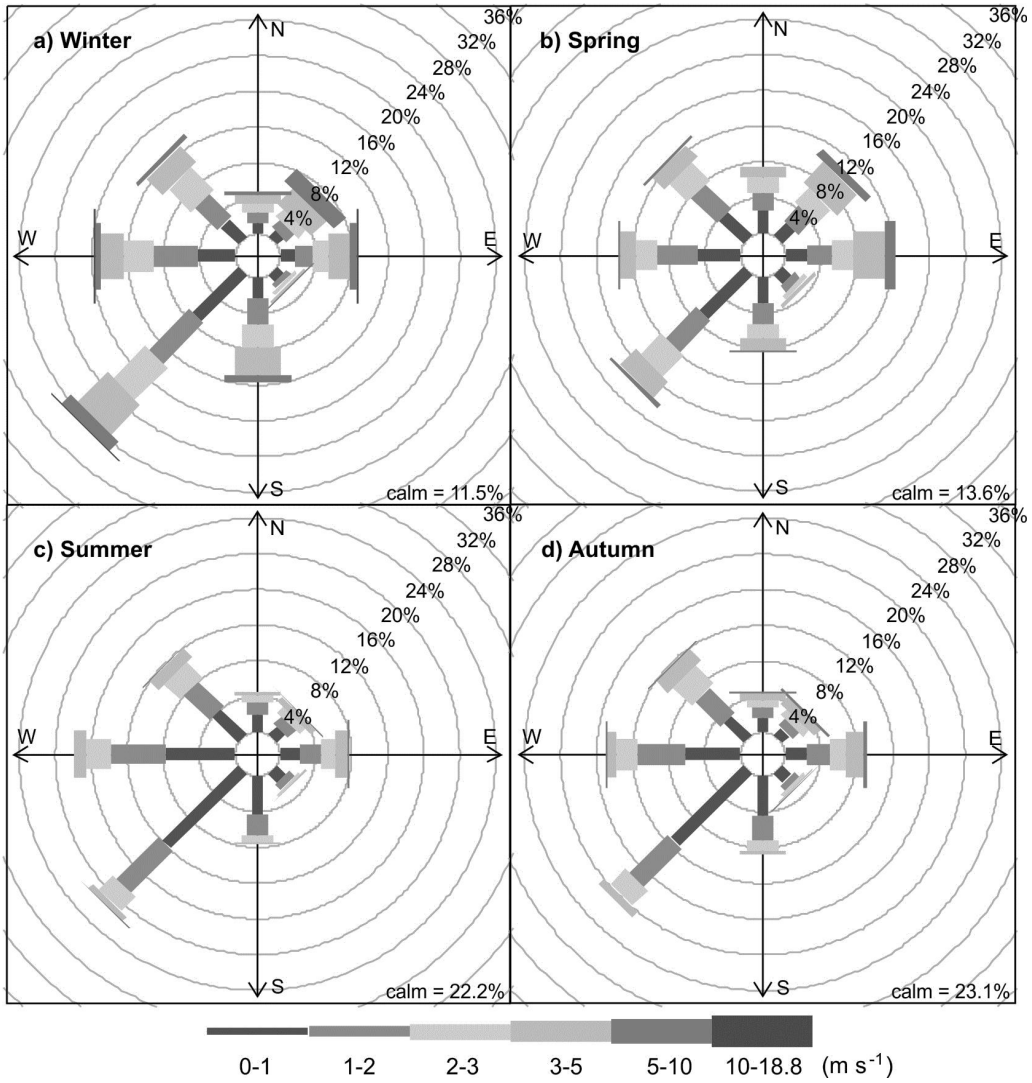

Figure 2. Frequency of counts of measured wind direction occurrence by season at the EGH site.

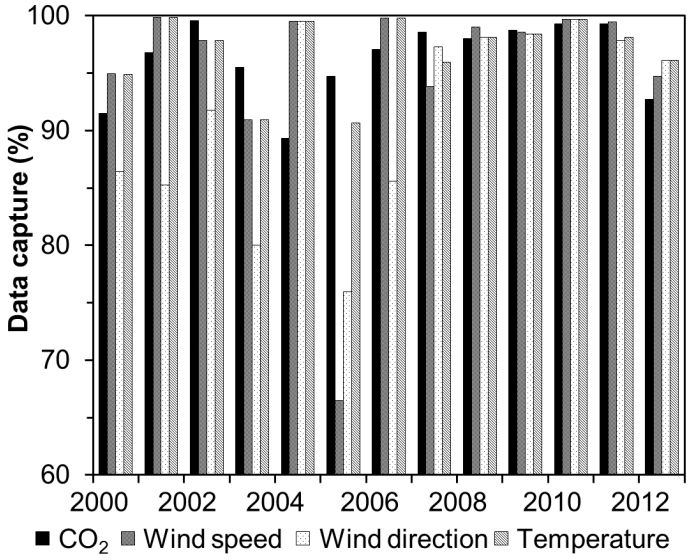

Figure 3. Data capture of 30-min values recorded for CO_2, wind speed, wind direction and temperature over 2000-2012 at EGH.

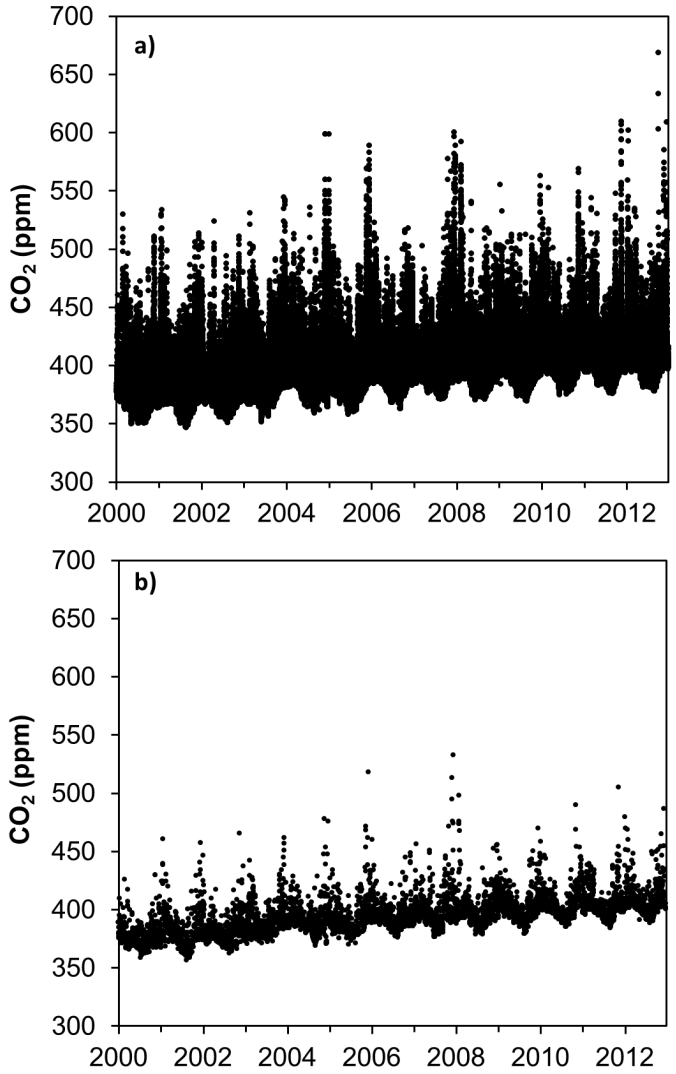

630

631 Figure 4a). 30-minute averages of atmospheric CO_2 recorded from Jan 2000 to Dec 2012 at
632 EGH. b). Daily averages during the same period.

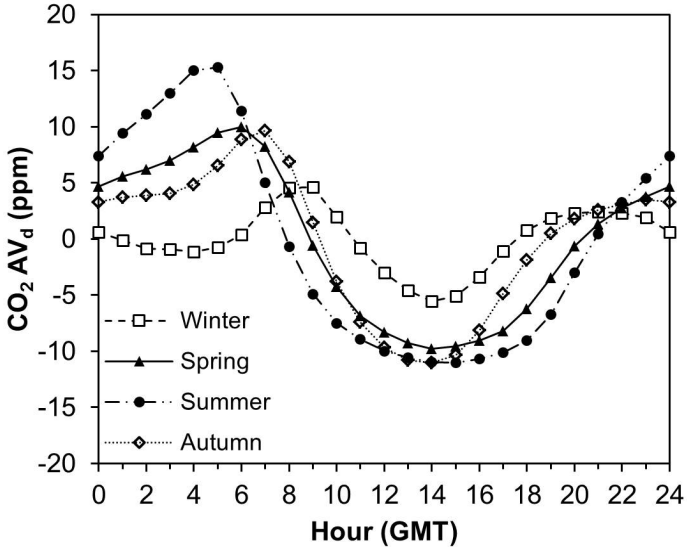

633
634 Figure 5. CO_2 de-trended daily cycles by season observed at the EGH site.

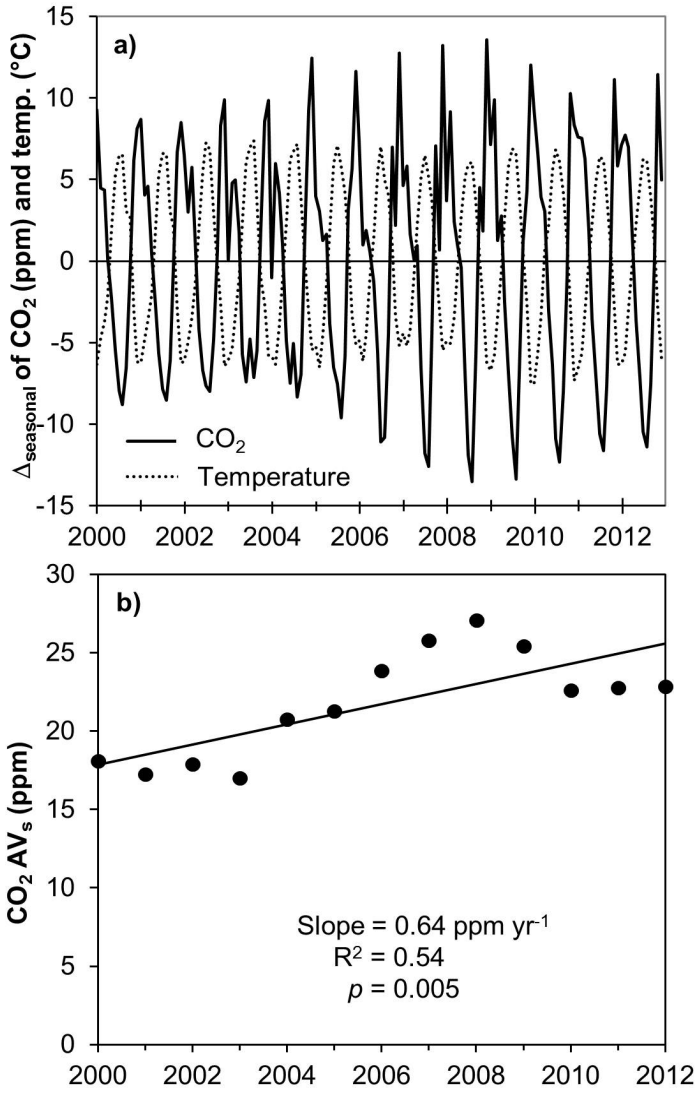

Figure 6a). Seasonal cycles of CO_2 constructed from filtered data using the STL technique developed by Cleveland et al. (1990). b). Seasonal amplitudes and trend of CO_2 at EGH from 2000 to 2012 .

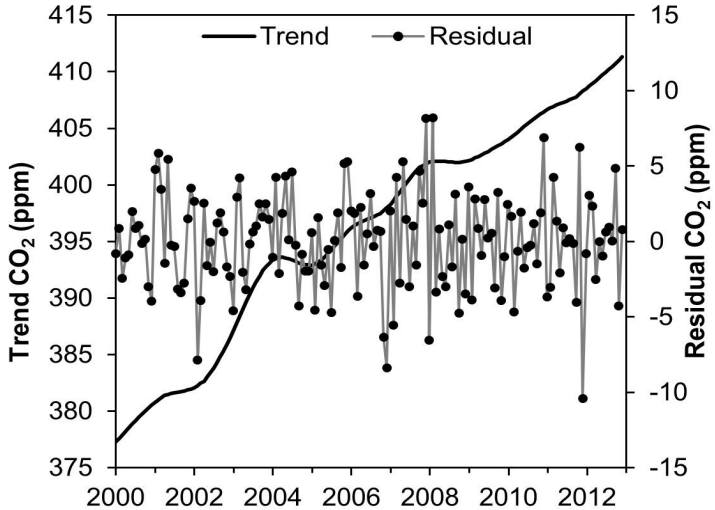

Figure 7. Smoothed trend and residuals of monthly CO_2 averages recorded at EGH from 2000 to 2012 computed with the STL technique developed by Cleveland et al. (1990).

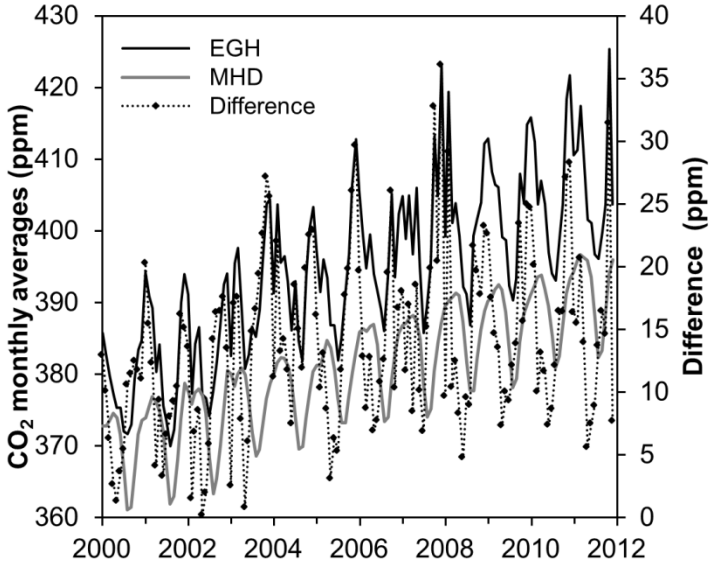

Figure 8. Comparison of monthly averages of CO_2 for EGH and MHD during 2000-2011. Monthly averages were calculated from daily averages.

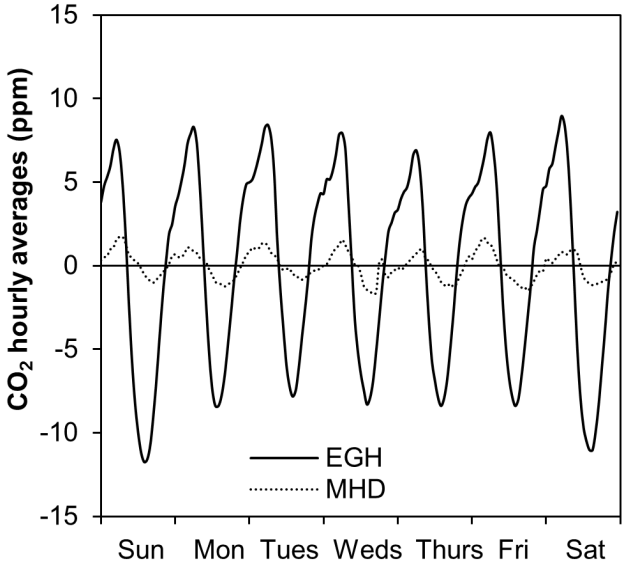

Figure 9. Normalised weekly cycles constructed from hourly averages at EGH and MHD during 2000-2011.

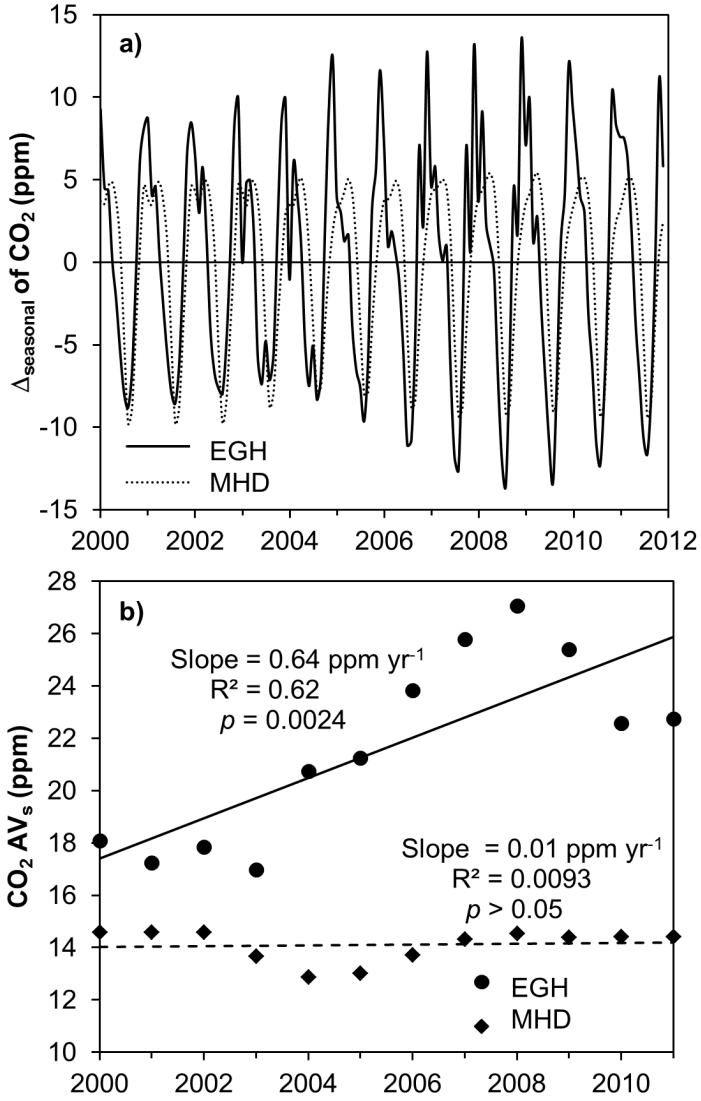

Figure 10a). Smoothed CO_2 seasonal cycles. b). Seasonal amplitudes observed at EGH and MHD monitoring sites from 2000 to 2011 calculated with the STL technique.

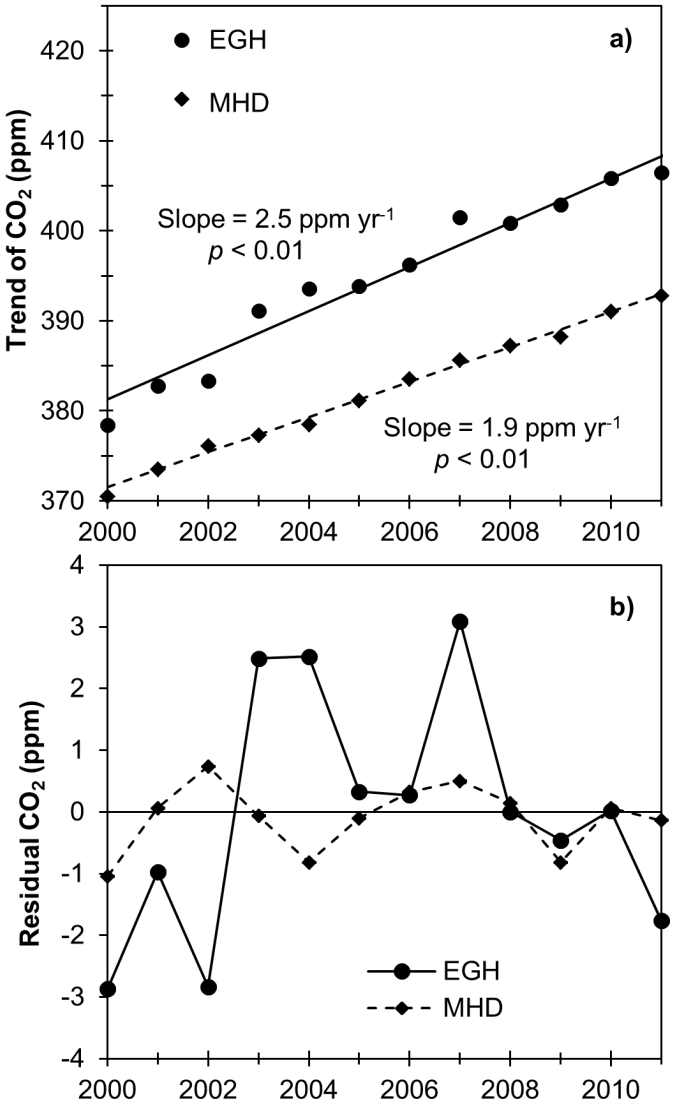

Figure 11a). CO_2 annual averages at EGH and MHD monitoring stations during 2000-2011; the lines represent the smoothed trend from the Mann-Kendall test. b). Annual residuals obtained from annual averages minus Sen's estimation.